iScience, Volume *23*

Supplemental Information

Nonmetallic Abiotic-Biological Hybrid Photocatalyst for Visible Water Splitting and Carbon Dioxide Reduction

Pier-Luc Tremblay, Mengying Xu, Yiming Chen, and Tian Zhang

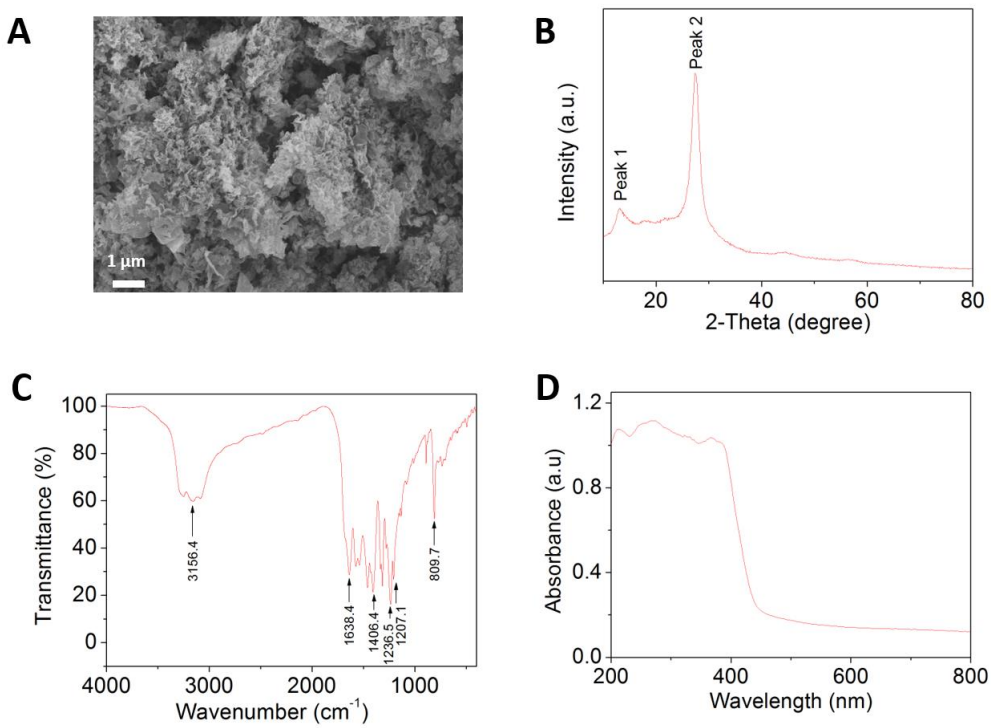

Figure S1. g-C_3N_4 characterization. (A) SEM image, **(B)** XRD, **(C)** FT-IR, and **(D)** UV-visible diffuse reflectance spectra of synthesized g-C_3N_4. X-ray diffraction (XRD) shows the two main characteristic peaks associated with g-C_3N_4. The first peak at 13.2° corresponds to tri-s-triazine units packing in the lattice planes parallel to the c axis. The second peak at 27.6° is attributed to the interlayer stacking of aromatic segments (Mao et al., 2017; Zang et al., 2014; Cheng et al., 2016). The Fourier transform infrared spectrum (FT-IR) includes skeletal vibrations in the range of 1200-1650 cm^{-1} for aromatic C-N heterocycles and a breathing vibration at 809.7 cm^{-1} for tri-s-triazine units characteristic of g-C_3N_4. Between 3000-3500 cm^{-1}, a broad absorption peak is observed corresponding to stretching vibrational modes of the O-H or N-H groups (Tang et al., 2015; Wang et al., 2017). The UV-visible light absorption spectrum is also typical of g-C_3N_4 with an upper limit at *ca.* 450 nm (Patnaik et al., 2017). Related to Figures 1, 2, and 3.

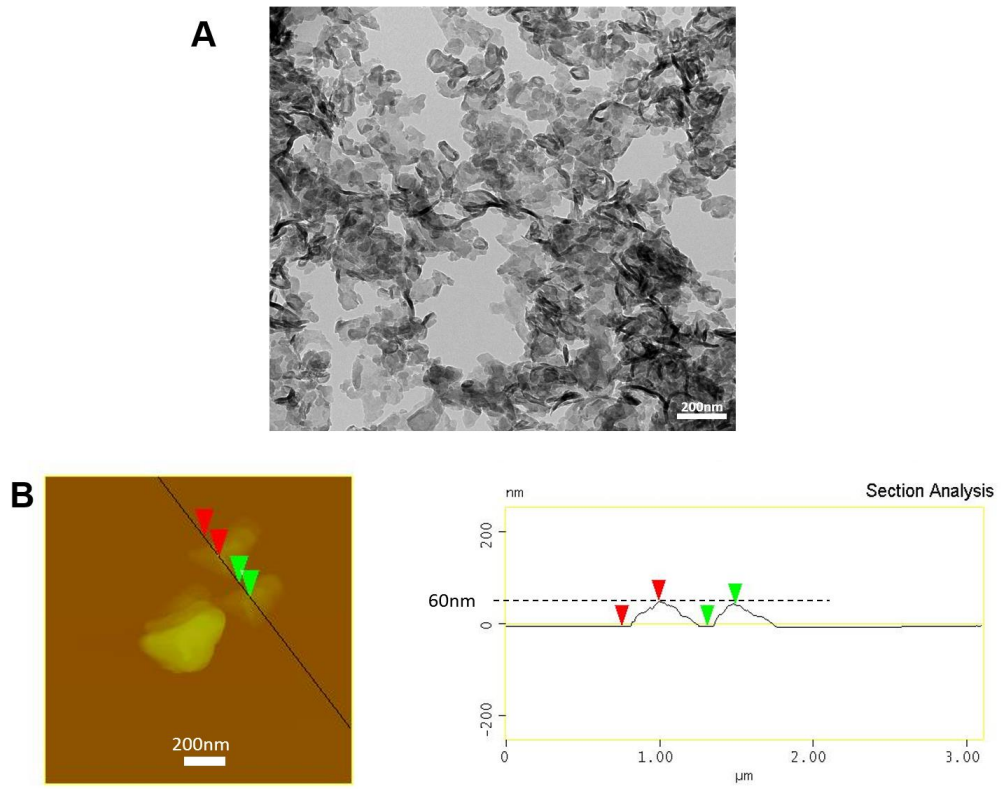

Figure S2. TEM and AFM analysis of g-C_3N_4 particles. (A) TEM image shows typical layered sheet-like structure of g-C_3N_4.[7] **(B)** Section analysis of the AFM image shows that the thickness of the g-C_3N_4 sheet-like particles was ca. 60 nm. Related to Figures 1, 2, and 3.

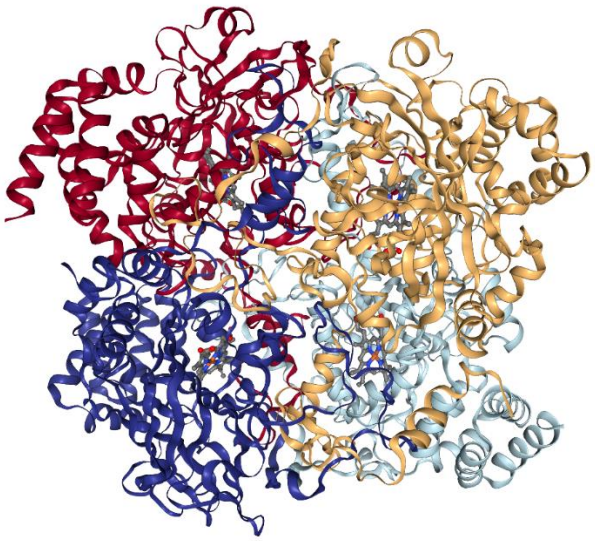

Figure S3. The crystal structure of the bovine liver catalase. The enzyme comprises four 60 kDa subunits. Each of these subunits contains an iron bound to a protoheme IX group (PDB ID: 1TGU; Sugadev, R., Balasundaresan, D., Ponnuswamy, M.N., Kumaran, D., Swaminathan, S., Sekar, K. The crystal structure of bovine liver catalase.). One unit of bovine liver catalase will degrade 1.0 μmole H_2O_2 min^{-1} at pH 7.0 at 25 °C according to the reaction $2H_2O_2 \rightarrow 2H_2O + O_2$. Related to Figures 3 and 4.

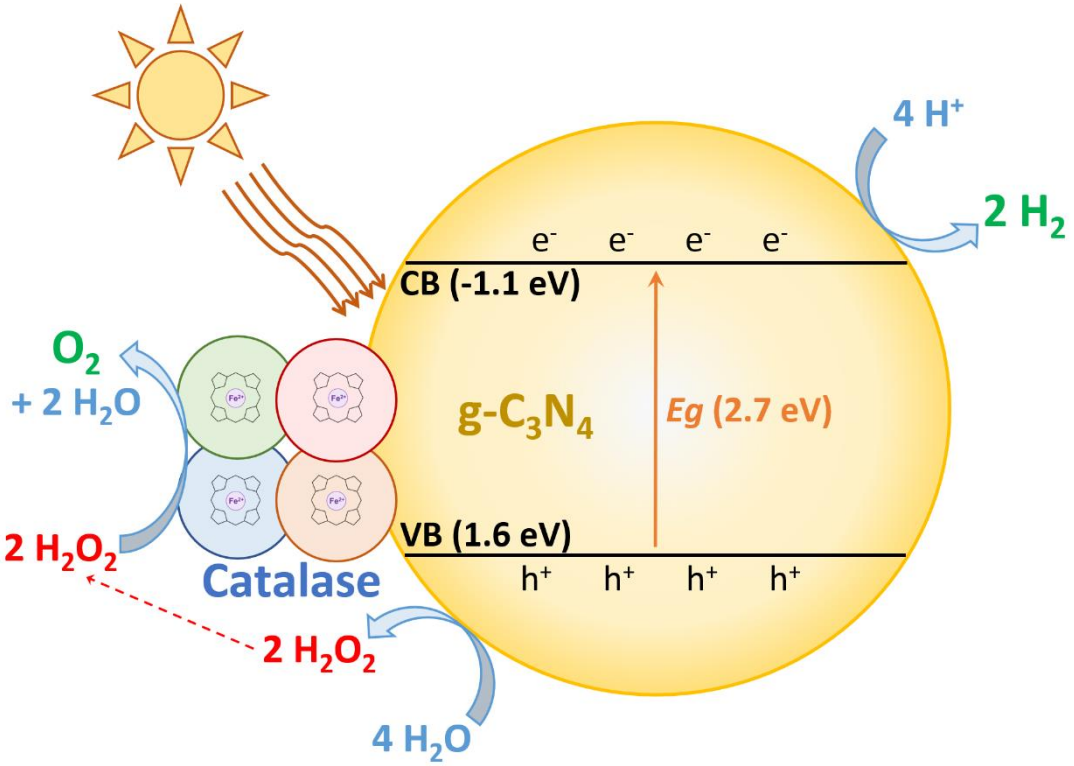

Figure S4. Schematic diagram of the g-C_3N_4-catalase enzymatic photocatalyst system. Water is oxidized to H_2O_2 by g-C_3N_4 under light. The bovine liver catalase decomposes H_2O_2 into O_2 and H_2O preventing H_2O_2 poisoning of g-C_3N_4. Concomitantly, protons are converted into H_2 by g-C_3N_4, thus completing the light-driven water-splitting reaction. CB: conduction band. VB: valence band. Related to Figures 3 and 4.

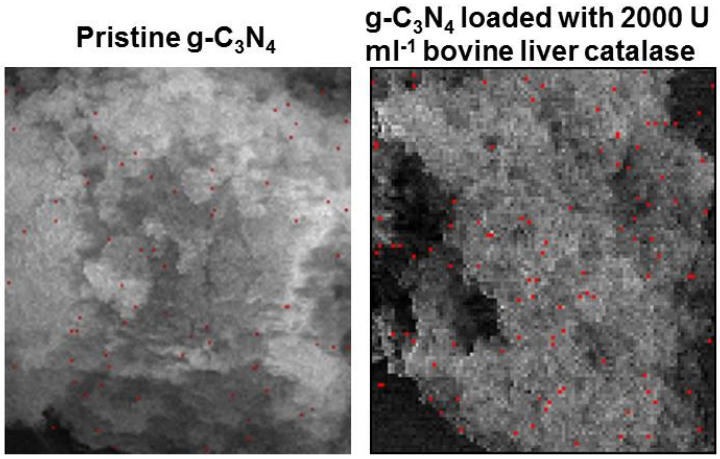

	Weight percentage	
Element	**Pristine g-C_3N_4**	**g-C_3N_4 with catalase**
Fe	0.18	1.74
C	38.90	40.22
N	60.93	58.04

Figure S5. SEM images of pristine g-C_3N_4 and g-C_3N_4 loaded with 2000 U mL^{-1} bovine liver catalase with iron elemental mapping and weight percentage for carbon, nitrogen, and iron. Elemental mapping and weight percentage were examined by energy dispersive X-Ray spectroscopy (EDS). Red dots on SEM images correspond to iron elements. Iron elements are bound to the four protoheme IX groups attached to the bovine liver catalase. Increased iron element weight percentage indicates the presence of catalase in the vicinity of g-C_3N_4. Related to Figures 3 and 4.

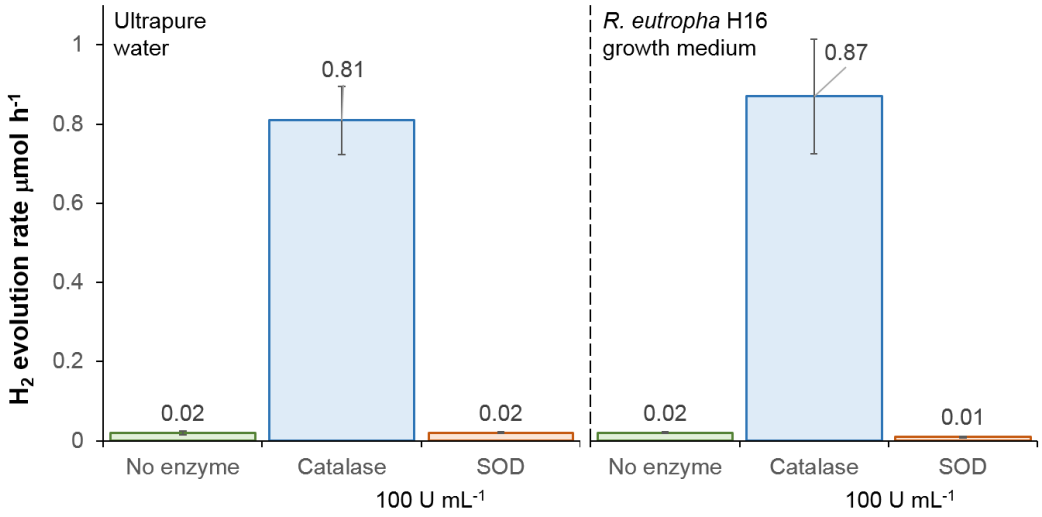

Figure S6. Light-driven water-splitting activity of g-C_3N_4 with catalase or SOD. Impact of 100 U mL^{-1} bovine liver catalase or SOD on H_2 evolution rate by g-C_3N_4 suspended in ultrapure water or *R. eutropha* growth medium under 4200 lux LED light. Each bar is the average of at least three replicates with standard deviation. Related to Figures 3 and 4.

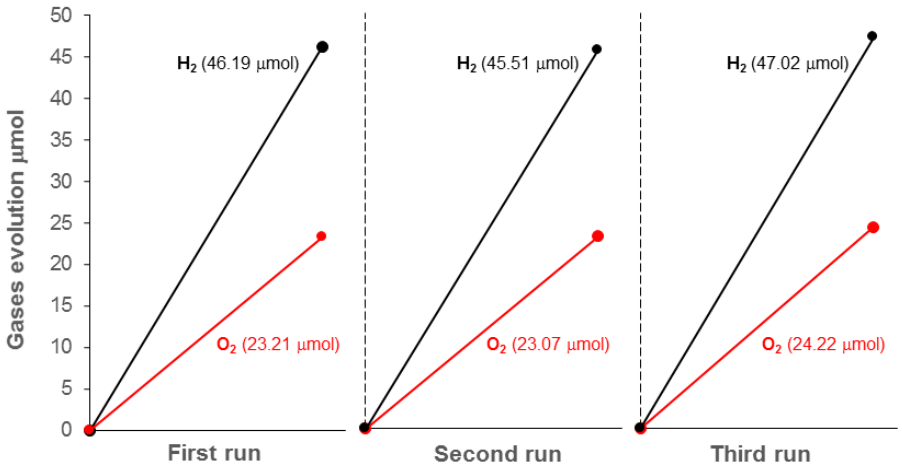

Figure S7. Cycling test for the g-C_3N_4-catalase PC system. H_2 and O_2 evolution by g-C3N4 with 10000 U mL^{-1} catalase under a light intensity of 200 W m^{-2} was monitored for several cycles of one hour. Related to Figures 3 and 4.

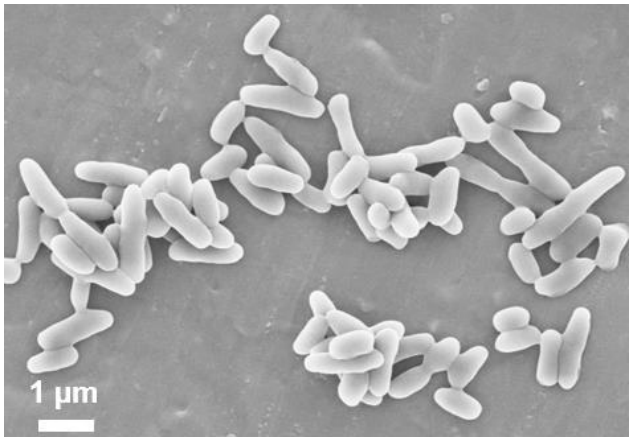

Figure S8. SEM image of *R. eutropha* H16 cells without g-C_3N_4. *R. eutropha* H16 is a Gram-negative rod-shape bacterium of the *Burkholderiaceae* family. *R. eutropha* H16 is also named *Cupriavidus necator* H16. Related to Figures 5 and 6.

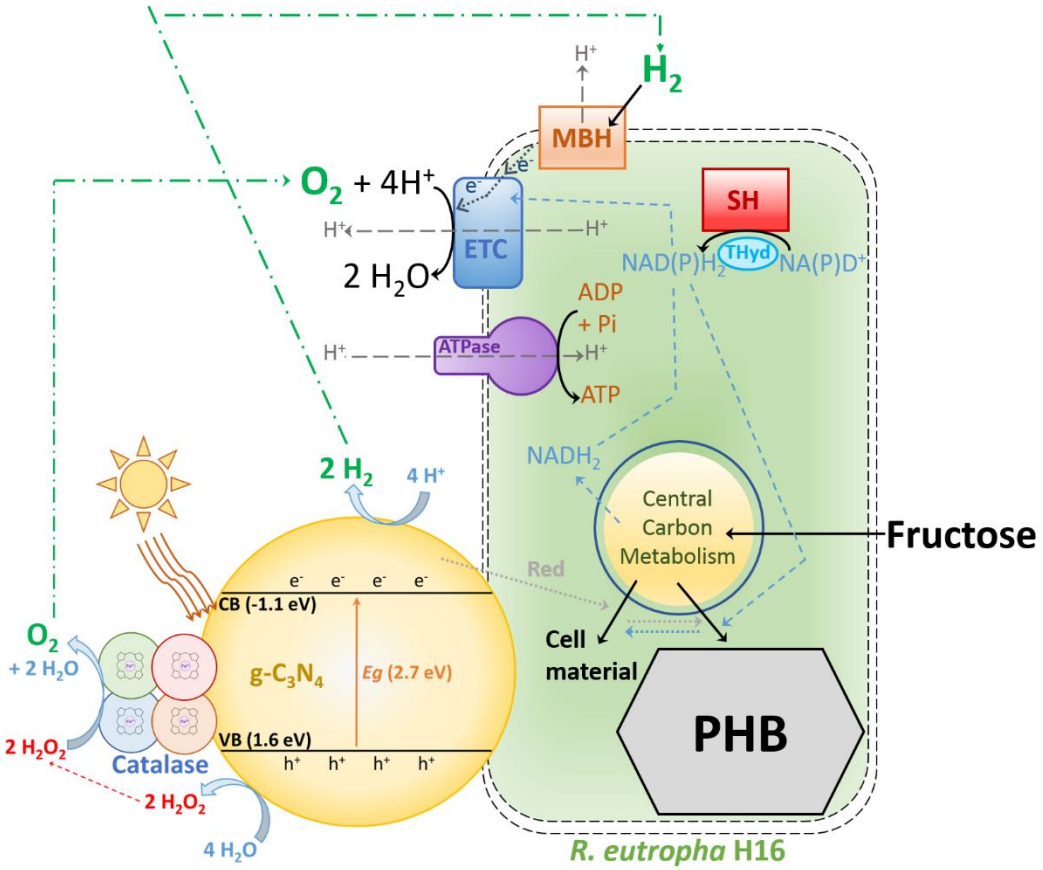

Figure S9. Schematic diagram of heterotrophic hybrid photosynthesis with g-C_3N_4-catalase and *R. eutropha* producing PHB from fructose. Water-splitting g-C_3N_4-catalase augments heterotrophic PHB production either by providing H_2 and/or O_2 molecules for the bacterial metabolism or by transferring unknown reducing equivalents (Red) to *R. eutropha*. ETC: electron transport chain. MBH: membrane-bound hydrogenase. SH: soluble hydrogenase. Thyd: $NAD(P)^+$ transhydrogenase. Related to Figure 6.

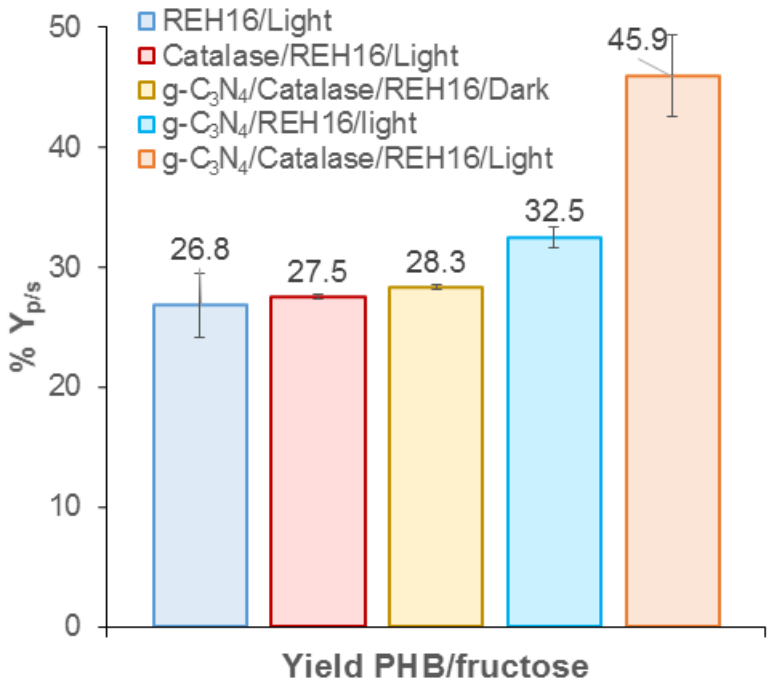

Figure S10. Impact of water-splitting g-C_3N_4-catalase on PHB to fructose yield of heterotrophically-grown *R. eutropha*. Yield gram PHB produced per gram fructose consumed ($Y_{p/s}$) after 96 hours of growth. REH16: *R. eutropha* H16. Each bar is the mean of at least three replicates with standard deviation. Related to Figure 6.

Table S1. Gene in *R. eutropha* H16 coding for H_2O_2-degrading enzyme catalase and peroxidase.[a]

Gene/locus	Annotation
Catalase	
katE1/H16_A3109	Catalase KatE1
katE2/H16_B1428	Catalase KatE2
katG/H16_A2777	Catalase (peroxidase I) KatG
Peroxidase	
H16_B0946	Predicted iron-dependent peroxidase
tpx/H16_A3175	Thiol peroxidase Tpx
H16_A3102	Glutathione peroxidase
H16_A0065	Glutathione peroxidase
H16_A3267	Peroxiredoxin
H16_A1460	Peroxiredoxin

[a]Related to Figure 2.

Table S2. Metal-free g-C_3N_4-based particulate photocatalyst systems splitting water under visible light.[a]

System	Performance	Comments	Reference
g-C_3N_4 with carbon nanodots	H_2 evolution: 191.7 μmol h^{-1} O_2 evolution: nearly stoichiometric STH[b]:2.0%	-80 mg PC[c] in 150 ml ultrapure water -AM 1.5G solar simulator	Liu et al., 2015
carbon-rich g-C_3N_4	H_2 evolution: 530 μmol h^{-1} g^{-1} catalyst O_2 evolution: nearly stoichiometric STH: Not reported	-30 mg PC in 80 ml distilled water -300 W Xe lamp (≥ 300 nm)	Fang et al., 2019
g-C_3N_4-catalase	H_2 evolution: 55.72 μmol h^{-1} O_2 evolution: nearly stoichiometric STH: 3.40% (200 W m^{-2})[d] and 1.00% (800 W m^{-2})[d]	-30 mg PC in 20 ml CAT buffer[e] -500 W Xe lamp with an AM1.5G filter	This work

[a]Related to Figure 4.

[b]STH: Solar-to-H_2 efficiency.

[c]PC: photocatalyst.

[d]Light intensity.

[e]CAT buffer: 50 mM KH_2PO_4 pH 7.4.

Table S3. Hybrid photosynthesis system with particulate photocatalyst for CO_2 reduction.[a]

Particulate photocatalyst	**Microbe**	**Comments**	**Reference**
CdS nanoparticles	*Moorella thermoacetica*	-Cysteine as sacrificial e^- donor -*Ca.* 1.1 mM acetate produced in 36 hours	Sakimoto et al., 2016a
CdS and TiO_2 nanoparticles	*M. thermoacetica*	-Z-scheme, water splitting -Cysteine as e^- shuttle -cocatalyst MnPc -*Ca.* 0.8 mM acetate produced in one day	Sakimoto et al., 2016b
CdS nanoparticles	*Methanosarcina barkeri*	-Cysteine as sacrificial e^- donor - 0.19 μmol h^{-1} methane	Ye et al., 2019
CdS nanoparticles	*Rhodopseudomonas palustris*	-Cysteine as sacrificial e^- donor -Biomass, carotenoids and polyhydroxybutyrate (PHB) production was increased to 148%, 122%, and 147%	Wang et al., 2019
g-C_3N_4	*Ralstonia eutropha* H16	-Water splitting -1.5-fold increase of PHB production	This work
g-C_3N_4 with catalase	*R. eutropha* H16	-Water splitting -2.2-fold increase of PHB production	This work

[a]Related to Figure 5.

TRANSPARENT METHODS

g-C_3N_4 preparation

g-C_3N_4 particles were prepared by a facile thermal treatment of urea as described previously (Liu et al., 2011). 10 g urea was placed into a semi-closed quartz crucible and then calcined in a muffle furnace for two hours with a heating rate of 10 °C min^{-1} up to 550 °C. The bulk product was filtered and washed three times with 20 mL 0.1 M HNO_3 and then washed five times with 20 mL ultrapure water to remove impurities from the sample surface. g-C_3N_4 was then dried at 55 °C for 24 h and ground into powder.

g-C_3N_4 characterization

The characterization of g-C_3N_4 was done with X-ray powder diffraction (XRD), Fourier-transform infrared spectroscopy (FT-IR), and UV-visible diffuse reflectance spectroscopy. The XRD spectrum of g-C_3N_4 was recorded within the scan range of 2θ from 10^0 to 80^0 using a D8 ADVANCE powder X-ray diffractometer (Bruker, MA, USA) equipped with Cu Kα X-ray. The FT-IR spectrum of g-C_3N_4 was obtained with a Nicolet iS5 FT-IR spectrometer (Thermo Fisher Scientific, MA, USA) using the KBr pellet method within the 400–4000 cm^{-1} range at a 0.8 cm^{-1} resolution. The UV-Visible diffuse reflectance absorption spectrum of the photocatalyst (PC) was recorded with a Lambda 750s spectrophotometer (PerkinElmer, MA, USA).

Bacterial strain and growth medium

The bacterium *R. eutropha* H16 (DSM-428) was used for this study. All bacterial cultures were grown at 30 ^{0}C in a nitrogen-limiting minimal medium, which has a pH of 6.8 (Budde et al., 2010). Components of the minimal medium per liter of ultrapure water are: 1 mL L^{-1} trace mineral mix, 1 g L^{-1} NH_4Cl, 5.2 g L^{-1} $NaH_2PO_4 \cdot 2H_2O$, 11.6 g L^{-1} $Na_2HPO_4 \cdot 12H_2O$, 0.45 g L^{-1} K_2SO_4, 0.8 g L^{-1} $MgSO_4 \cdot 7H_2O$, and 0.08 g L^{-1} $CaCl_2 \cdot 2H_2O$. Components of the trace mineral mix per liter of 0.1 M HCl are: 15 g L^{-1} $FeSO_4 \cdot 7H_2O$, 2.4 g L^{-1} $MnSO_4 \cdot H_2O$, 2.4 g L^{-1} $ZnSO_4 \cdot 7H_2O$, and 0.48 g L^{-1} $CuSO_4 \cdot 5H_2O$.

Under heterotrophic conditions, *R. eutropha* was grown in flasks containing 50 mL minimal medium with 20 g L^{-1} fructose. Under autotrophic conditions, *R. eutropha* H16 was grown in rubber stopper-sealed serum bottles containing 100 mL fructose-free minimal medium under a N_2:H_2:O_2:CO_2 (49:37:7:7) atmosphere.

Cell-free spent medium preparation, pronase treatment, H_2O_2-degrading enzymatic activity, and total protein concentration

For cell-free spent medium preparation, a *R. eutropha* culture grown with fructose for 40 hours was centrifuged at 10000 x g for 10 minutes at 4 ^{0}C. The supernatant was collected and centrifuged for a second time to ensure the complete removal of *R. eutropha* cells. The supernatant from the second centrifugation was considered as cell-free spent medium. For protein degradation treatment, 1 mg mL^{-1} pronase was added to

the cell-free spent medium, which was then incubated overnight at 37 ^{0}C. Total protein concentration in cell-free spent medium was measured with the M5 BCA protein assay kit (Mei5 Biotechnology, China).

H_2O_2-degrading enzymatic activity was measured as described before with several modifications (Beers and Sizer, 1952). 10 mM H_2O_2 was added into sterile minimal medium or cell-free spent medium pre-incubated at 30 ^{0}C. 400 μL of the reaction was quickly transferred to a quartz cuvette and absorbance at 240 nm was monitored over time with an Evolution 220 UV-Visible spectrophotometer (Thermo Fisher Scientific, USA). H_2O_2 concentration was calculated according to equation (1).

$$A = \varepsilon cl \qquad (1)$$

Where A is the absorbance, c is the concentration, l is the light path length (1 cm), and ε is the molar extinction coefficient, which is 43.6 M^{-1} cm^{-1} for H_2O_2 at a wavelength of 240 nm.

Photocatalytic H_2, O_2, and H_2O_2 evolution under a 4200 lux LED light

The photocatalytic evolution experiments of H_2, O_2, and H_2O_2 were carried out in rubber stopper-sealed 120 mL serum bottles incubated at 30 ^{0}C into a CZL-P280D LED light incubator (Hua De Li, China) set at 4200 lux. Serum bottles contained 10 mg g-C_3N_4 particles dispersed in 20 mL ultrapure water, 50 mM KH_2PO_4 buffer pH 7.4

(CAT), sterile minimal medium, or cell-free spent medium. Where indicated, 10, 100, 500, or 2000 U mL^{-1} bovine liver catalase (Yuan Ye, China) or 100 U mL^{-1} superoxide dismutase (Yuan Ye) was added to the PC suspension. Prior to photocatalytic experiments, g-C_3N_4 suspensions were flushed with pure nitrogen for 20 minutes. Where indicated, 5% (w/v) triethanolamine (TEOA) was added to the PC suspension.

H_2 and O_2 were measured with a GC9720 Plus gas chromatograph (FULI, China) equipped with a 5A molecular sieve column and a thermal conductivity detector (TCD). For H_2O_2 measurement, 1 mL g-C_3N_4 suspension was sampled and centrifuged at 7000 x g for 1 minute. The top 400 µl of the supernatant was transferred to a quartz spectrophotometer cuvette and H_2O_2 concentration was measured at 240 nm.

g-C_3N_4-catalase activity under a solar simulator

The photocatalytic activity of g-C_3N_4 suspended in CAT buffer containing 2000, 5000, or 10000 U mL^{-1} bovine liver catalase was evaluated at room temperature under a PL-XQ 500 W Xe lamp (Pu Lin Sai Si, China) equipped with an air mass 1.5 global conditions filter (AM1.5G) with a light intensity of 200 W m^{-2} or 800 W m^{-2} (ca. 0.2 to 0.8 sun). For quantum efficiency (QE_{420nm}) determination, the Xe lamp was instead equipped with a band-pass filter of 420 ± 20 nm. The intensity of the light reaching g-C_3N_4-catalase was measured with a TES-132 light radiometer (TES, China). Nitrogen-flushed serum bottles with g-C_3N_4-catalase were prepared as described above with the exception that 30 mg PC was in suspension instead of 10 mg. For the cycling test, H_2

and O_2 evolution by g-C_3N_4 were measured three times with 10000 U mL^{-1} catalase under a light intensity of 200 W m^{-2}. Between each run, the headspace of the serum bottle was flushed 20 minutes with pure nitrogen.

Solar-to-hydrogen efficiency and quantum efficiency calculations

The solar-to-hydrogen (STH) efficiency was evaluated with the 500 W Xe lamp equipped with an AM1.5G filter according to equation (2).

$$\text{STH \%} = 100E_{H_2} / Es\ A \text{ or } 100\Delta G^0_{H_2} R_{H_2} / Es\ A \qquad (2)$$

Where E_{H_2} is the energy stored in H_2, Es is the light energy radiation per m^2 per second (J m^{-2} s^{-1}), A is the illumination area in m^2, $\Delta G^0_{H_2}$ is the standard Gibbs energy of 237200 J mol^{-1} at 297 K for the energy storage reaction generating H_2, and R_{H_2} is the H_2 evolution rate in mol s^{-1}.

QE_{420nm} was calculated according to equations (3) and (4).

QE_{420nm} % =

2 x number of evolved H_2 molecules / number of incident photons x 100 (3)

$$\text{Number of incident photons} = IAt\lambda / hc \qquad (4)$$

Where I is the light intensity in W m^{-2}, A is the illumination area in m^2, t is the time in second, λ is the wavelength, h is the Planck constant $6.626x10^{-34}$ J s, and c is the speed of light $3x10^8$ m s^{-1}.

Hybrid photosynthesis with *R. eutropha* and g-C_3N_4-catalase

For autotrophic hybrid photosynthesis, *R. eutropha* grown to mid-log with CO_2 as sole carbon source was used as inoculum. A serum bottle containing 100 mL minimal medium with 0.5 g L^{-1} g-C_3N_4 and 5000 U mL^{-1} bovine liver catalase under a N_2:H_2:CO_2:O_2 atmosphere was inoculated with CO_2-grown *R. eutropha* at an initial optical density (OD_{600nm}) of 0.01, and then it was incubated at 30 ^{0}C under LED light at an intensity of 4200 lux. PHB production was monitored during 48 hours. For heterotrophic hybrid photosynthesis, a fructose-grown *R. eutropha* mid-log culture was used to inoculate a flask containing 0.5 g L^{-1} g-C_3N_4 and 5000 U mL^{-1} bovine liver catalase in 50 mL minimal medium with 20 g L^{-1} fructose. The initial OD_{600nm} was 0.05. Both PHB production and fructose consumption were monitored over 96 hours for the heterotrophic g-C_3N_4-catalase-*R. eutropha* system, which was incubated at 30 °C under LED light at an intensity of 4200 lux. Controls without g-C_3N_4, catalase, or light exposure were also tested for PHB production.

PHB, fructose, and production yield

PHB was extracted and measured as described previously (Xu et al., 2019; Braunegg et al., 1978). 10 mL of PHB-containing samples were centrifuged at 7000 x g for 10 minutes at 4 °C. Cell pellets were washed twice with ultrapure water before being dried overnight at 55 °C. Samples were added to 2 mL methanol acidified with 3% (v/v)

H_2SO_4. Extraction mixtures were then incubated for 4 hours in screw-capped glass tubes at 100 ^{0}C. After cooling of the samples at room temperature, 1 mL ultrapure water was added to the extraction mixtures, which were then shaken vigorously for 1 minute. The organic phase was removed after separation from the aqueous phase and transferred to a glass vial. Extracted PHB in the organic phase was measured with a GC9720 gas chromatograph (Fuli) equipped with a RB-FFAP column and a flame ionization detector (FID). The gas chromatograph column was maintained at an initial temperature of 50 °C for 2 minutes with subsequent temperature increase rate of 10 ^{0}C min^{-1} up to 220 ^{0}C for 2 minutes.

Fructose concentration was measured with a Breeze 2 high-performance liquid chromatograph (Waters, MA, USA) equipped with a Refractive Index Detector and an Aminex HPX-87H anion exchange column (Bio-Rad, CA, USA) set at a temperature of 50 °C. The mobile phase was 5 mM H_2SO_4 at a flow rate of 0.6 ml min^{-1}. Yield of PHB production to fructose consumption is calculated according to equation (5).

$Y_{p/s}$ = grams PHB ($[C_4H_6O_2]n$) produced / grams fructose ($C_6H_{12}O_6$) consumed (5)

Microscopy and energy-dispersive X-ray diffraction

The structure of g-C_3N_4 particles was characterized by SEM, TEM, and atomic force microscopy (AFM). Elemental mapping of g-C_3N_4 samples with or without 2000 U mL^{-1} bovine liver catalase was completed by energy dispersive X-ray spectroscopy (EDS).

Both SEM and EDS were performed with a S-4800 Field-emission scanning electron microscope (Hitachi, Japan). Samples were dropped on a silicon wafer and air-dried before being scanned at an accelerating voltage of 5 kV. For TEM, g-C_3N_4 samples were dispersed into ethanol by ultrasonic treatment and diluted before being dropped on a copper grid. TEM images were obtained with a JEM-1400Plus (JEOL, Japan) microscope at an accelerating voltage of 120 kV. AFM analysis was performed with a Nanoscope IV (Veeco, NY).

For SEM of hybrid photosynthesis system, 24-hours autotrophic or heterotrophic bacterial cultures with g-C_3N_4-catalase were collected and fixed overnight at 4 ^{0}C in a 0.1 M Na phosphate buffer (pH 7.0) containing 2.5% glutaraldehyde. Samples were then washed one time serially with 30%, 50%, 70%, 80%, 90% ethanol and two times with 100% ethanol. Samples suspended in 100% ethanol were dropped on a silicon wafer and air-dried, and then they were scanned at an accelerating voltage of 5 kV. The same procedure was employed to prepare the hybrid photosynthesis samples for TEM with the exception that g-C_3N_4-catalase with *R. eutropha* H16 was dropped on a copper grid instead of silicon wafer.

Electrochemical impedance spectroscopy (EIS)

Photoelectrochemical measurements were conducted with a CHI600E potentiostat (CH Instruments, TX, USA) using a three-electrode system with *R. eutropha* autotrophic growth medium as electrolyte. A glassy carbon electrode (diameter of 3 mm) served as

the working electrode, a platinum sheet was used as the counter electrode, and an Ag/AgCl electrode (3.5 M KCl) was employed as the reference electrode. EIS spectra were acquired with a sinusoidal perturbation of 5 mV amplitude and frequencies ranging from 100 kHz to 0.1 Hz at -1.2 V versus Ag/AgCl under illumination.

REFERENCES

Beers, R.F., and Sizer, I.W. (1952). A spectrophotometric method for measuring the breakdown of hydrogen peroxide by catalase. J. Biol. Chem. *195*, 133–140.

Braunegg, G., Sonnleitner, B., and Lafferty, R.M. (1978). A rapid gas chromatographic method for the determination of poly-β-hydroxybutyric acid in microbial biomass. European J. Appl. Microbiol. Biotechnol. *6*, 29–37.

Budde, C.F., Mahan, A.E., Lu, J., Rha, C., and Sinskey, A.J. (2010). Roles of multiple acetoacetyl coenzyme A reductases in polyhydroxybutyrate biosynthesis in *Ralstonia eutropha* H16. J. Bacteriol. *192*, 5319–5328.

Cheng, R., Fan, X., Wang, M., Li, M., Tian, J., and Zhang, L. (2016). Facile construction of $CuFe_2O_4$/g-C_3N_4 photocatalyst for enhanced visible-light hydrogen evolution. RSC Adv. *6*, 18990–18995.

Fang, X., Gao, R., Yang, Y., and Yan, D. (2019). A cocrystal precursor strategy for carbon-rich graphitic carbon nitride toward high-efficiency photocatalytic overall water splitting. iScience *16*, 22–30.

Liu, J., Zhang, T., Wang, Z., Dawson, G., and Chen, W. (2011). Simple pyrolysis of urea into graphitic carbon nitride with recyclable adsorption and photocatalytic activity. J. Mater. Chem. *21*, 14398–14401.

Liu, J., Liu, Y., Liu, N., Han, Y., Zhang, X., Huang, H., Lifshitz, Y., Lee, S.-T., Zhong, J., and Kang, Z. (2015). Metal-free efficient photocatalyst for stable visible water splitting via a two-electron pathway. Science *347*, 970–974.

Mao, Z., Chen, J., Yang, Y., Wang, D., Bie, L., and Fahlman, B.D. (2017). Novel g-C_3N_4/CoO nanocomposites with significantly enhanced visible-light photocatalytic activity for H_2 evolution. ACS Appl. Mater. Interfaces *9*, 12427–12435.

Patnaik, S., Martha, S., Madras, G., and Parida, K. (2016). The effect of sulfate pre-treatment to improve the deposition of Au-nanoparticles in a gold-modified sulfated g-C_3N_4 plasmonic photocatalyst towards visible light induced water reduction reaction. Phys. Chem. Chem. Phys. *18*, 28502–28514.

Sakimoto, K.K., Wong, A.B., and Yang, P. (2016a). Self-photosensitization of nonphotosynthetic bacteria for solar-to-chemical production. Science *351*, 74–77.

Sakimoto, K.K., Zhang, S.J., and Yang, P. (2016b). Cysteine–Cystine Photoregeneration for Oxygenic Photosynthesis of Acetic Acid from CO_2 by a Tandem Inorganic–Biological Hybrid System. Nano Lett. *16*, 5883–5887.

Tang, C., Liu, E., Fan, J., Hu, X., Ma, Y., and Wan, J. (2015). A graphitic-C_3N_4-hybridized Ag_3PO_4 tetrahedron with reactive {111} facets to enhance the visible-light

photocatalytic activity. RSC Adv. *5*, 91979–91987.

Wang, Q., Guan, S., and Li, B. (2017). 2D graphitic-C_3N_4 hybridized with 1D flux-grown Na-modified $K2Ti_6O_{13}$ nanobelts for enhanced simulated sunlight and visible-light photocatalytic performance. Catal. Sci. Technol. *7*, 4064–4078.

Wang, B., Jiang, Z., Yu, J.C., Wang, J., and Wong, P.K. (2019). Enhanced CO_2 reduction and valuable C_{2+} chemical production by a CdS-photosynthetic hybrid system. Nanoscale *11*, 9296–9301.

Xu, M., Tremblay, P.-L., Jiang, L., and Zhang, T. (2019). Stimulating bioplastic production with light energy by coupling *Ralstonia eutropha* with the photocatalyst graphitic carbon nitride. Green Chem. *21*, 2392–2400.

Ye, J., Yu, J., Zhang, Y., Chen, M., Liu, X., Zhou, S., and He, Z. (2019). Light-driven carbon dioxide reduction to methane by *Methanosarcina barkeri*-CdS biohybrid. Appl. Catal. B *257*, 117916.

Zang, Y., Li, L., Xu, Y., Zuo, Y., and Li, G. (2014). Hybridization of brookite TiO_2 with g-C_3N_4: a visible-light-driven photocatalyst for As^{3+} oxidation, MO degradation and water splitting for hydrogen evolution. J. Mater. Chem. A *2*, 15774–15780.